CHEMISTRY
A EUROPEAN JOURNAL

Metal-Directed Synthesis and Photophysical Studies of Trinuclear V-Shaped and Pentanuclear X-Shaped Ruthenium and Osmium Metallorods and Metallostars Based upon 4′-(3,5-Dihydroxyphenyl)-2,2′:6′,2″-terpyridine Divergent Units

Edwin C. Constable,*[a] Robyn W. Handel,[a] Catherine E. Housecroft,[a] Angeles Farràn Morales,[b] Barbara Ventura,[b] Lucia Flamigni,[b] and Francesco Barigelletti*[b]

Abstract: A new series of V-shaped trinuclear metallorods and X-shaped pentanuclear metallostars has been prepared by the reaction of metal complexes bearing pendant phenolic functionalities with complexes containing electrophilic ligands. Specifically, {M(tpy)$_2$} motifs (M = Ru or Os; tpy = 2,2′:6′,2″-terpyridine) bearing one or two pendant 3,5-dihydroxyphenyl substituents at the 4-position of the central ring of the tpy have been reacted with the complexes [Ru(tpy)(Xtpy)]$^{2+}$ (X = Cl or Br) to form new ether-linked species. The energy transfer from ruthenium to osmium in these complexes has been investigated in detail and the efficiency of transfer shown to be highly temperature dependent; the energy transfer is highly efficient at low temperature, whereas at room temperature nonradiative and nontransfer deactivation of the excited {Ru(tpy)$_2$}* domains is most significant.

Keywords: dendrimers · nitrogen heterocycles · osmium · photochemistry · ruthenium

Introduction

Metallodendrimers may incorporate metal centres at various sites and a variety of synthetic methodologies have been devised for the efficient preparation of species in which metal–metal interactions may be fine-tuned, both with respect to their magnitude and their directionality.[1–3] We and others have been particularly interested in species in which luminescent ruthenium(II) and osmium(II) centres have been built into dendrimers and related species and have developed strategies for the preparation of a wide variety of multinuclear compounds based upon {M(tpy)$_2$} and {M(bpy)$_3$} motifs (tpy = 2,2′:6′,2″-terpyridine, bpy = 2,2′-bipyridine).[1–3] Particular interest has centred upon systems derived from multitopic ligands with multiple tpy metal-binding domains that lead to multinuclear species with multiple {M(tpy)$_2$} motifs; these have an advantage over compounds with multiple stereogenic {M(bpy)$_3$} motifs in that they give rise to monodisperse species rather than mixtures of diastereoisomers.[3–5] By controlling the relative spatial positioning and the nature of the chemical connectivity between the metal centres, it is possible to devise systems that generate designed structures showing controlled directional ruthenium-to-osmium energy transfer or electron transfer.[6] We have also drawn attention to the synthetic merits of metallostars (or first-generation metallodendrimers) in which there is a single branching point at the core.[1a,7] Such systems show minimal interactions between surface functional groups and are amenable to both divergent and convergent synthetic strategies.

Although a range of strategies for the synthesis of metallodendrimers have been developed, we and others have established a metal-directed approach as an efficient, general and facile method for the linking of metal-containing building blocks.[7,8] The basic strategy involves reactions at the organic component of metal complexes containing functional-

[a] Prof. Dr. E. C. Constable, Dr. R. W. Handel, Prof. Dr. C. E. Housecroft
Department of Chemistry, University of Basel
Spitalstrasse 51, 4056 Basel (Switzerland)
Fax: (+41) 61-267-1005
E-mail: edwin.constable@unibas.ch

[b] Dr. A. Farràn Morales, Dr. B. Ventura, Dr. L. Flamigni, Dr. F. Barigelletti
Istituto per la Sintesi Organica e Fotoreattività (ISOF-CNR)
Via P. Gobetti 101, 40129 Bologna (Italy)
Fax: (+39) 051-639-9844
E-mail: franz@isof.cnr.it

DOI: 10.1002/chem.200500119

ised heterocyclic ligands. The reaction of either free or coordinated ligands containing nucleophilic substituents with a complex containing an (activated) electrophilic ligand is used for the covalent linking of two metal centres through a new bridging ligand that is assembled in situ. This approach has been particularly useful in the preparation of complexes with ether bridges between the component metal-containing building blocks[9] and is also effective in the preparation of metallostars in which a core mononuclear electrophilic/nucleophilic zeroth-generation complex is functionalised by reaction with nucleophilic or electrophilic ligands or metal complexes, respectively. Convergent approaches in which bpy and tpy ligands with multiple metal-containing substituents are brought together by coordination to a metal at the core of the zeroth generation have also proved successful.[7,8]

The lowest-lying triplet states in ruthenium oligopyridine complexes lie about 0.2 eV higher in energy than in the corresponding osmium complexes and light-driven Ru→Os energy transfer is easily observed in heterometallic ruthenium(II)–osmium(II) systems.[6,9–12] In several such systems, the direction of the vectorial energy flow may be controlled by modifying the spatial arrangement of the Ru- and Os-based units, although a quantitative clarification of the rate constants is not always possible.[12] At room temperature, the pentanuclear and trinuclear tpy-based arrays reported herein are photoinert towards Ru→Os photoinduced energy transfer. However, their study at low temperature provides deep insights into the process: a practically complete Ru→Os energy conversion is observed at low temperature and the measured rate constants for energy transfer can be described in terms of a dipole–dipole transfer mechanism.[12]

Results and Discussion

Strategy: We planned a divergent approach to the synthesis of polynuclear complexes in which branching occurred in the zeroth generation at bifurcating substituents. In previous studies, we have used pentaerythritol cores and branching sites to prepare high nuclearity metallodendrimers based upon a connectivity of four.[5,13] In this paper, we describe the preparation of metallocentric systems in which the zeroth generation contains tpy metal-binding domains with pendant multiple phenolic substituents. The key expansion step in the synthesis involves the reaction of the pendant phenolate functionality with electrophilic metal complexes.

Our specific target was the bifurcating ligand 4′-(3,5-dihydroxyphenyl)-2,2′:6′,2″-terpyridine (**2**). This can bind a metal centre at the tpy domain and react with two electrophilic centres at the pendant phenolic sites. The difference in hardness of phenol/phenolate and pyridine nitrogen donors and the chelating character of the tpy domain ensure that all reactions are highly regioselective.

Ligand synthesis: We adopted a variation on the Kröhnke pyridine synthesis[14] for the preparation of **2** and considered it optimal to protect the phenolic substituents as methyl ethers through the ring synthesis. Subsequent deprotection of the methoxy groups can be achieved in high yield in tpy derivatives. The reaction of 2-acetylpyridine with 3,5-dimethoxybenzaldehyde proceeded smoothly in a sequential one-pot process involving treatment with KO*t*Bu in THF followed by ammonium acetate/acetic acid to give a satisfactory yield of the dimethoxy compound **1**.[15,16] Deprotection by heating with pyridinium chloride[16,17] gave the bifurcating ligand **2** in quantitative yield (Scheme 1). The new ligands **1** and **2** were fully characterised (see Experimental Section) and had the expected spectroscopic properties.

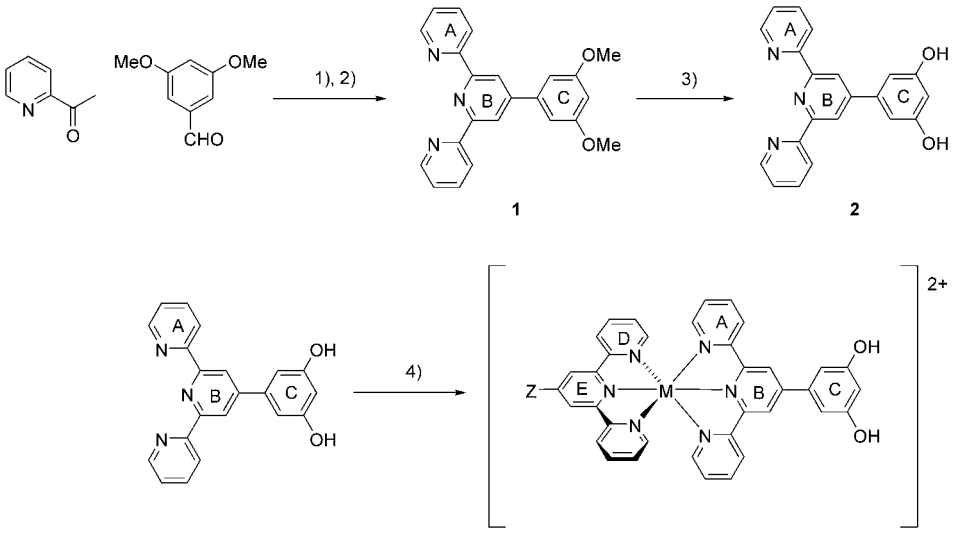

Scheme 1. Synthesis of the bifurcating ligand **2** and the core mononuclear complexes for the trinuclear complexes showing the ring-labelling scheme adopted. 1) KO*t*Bu, THF; 2) NH_4OAc, AcOH, EtOH, 54.5% yield; 3) pyridinium chloride, 210°C, quantitative yield; 4) $[M(Ztpy)Cl_3]$; M = Os or Ru, Z = H (ligand = tpy) or 2-thienyl (ligand = **5**). In the case of the complexes with ligand **5**, the thienyl ring is labelled F.

Synthesis of trinuclear complexes: One of our long-term aims is the construction of light-driven machines and for this we require bi- or polyfunctional systems in which light-collecting components are connected through energy- or electron-transfer processes to motifs that can subsequently perform chemical or electrochemical transformations. To this end, the $\{M(tpy)_2\}$ motif is attractive as one of the tpy ligands may be further functionalised with the light-absorbing components and the other with the conversion system (for example, a carboxylic acid for anchoring to a semiconductor

in Grätzel-type photovoltaic devices).[18] The key building blocks are the mononuclear complexes $[M(Ztpy)(\mathbf{2})]^{2+}$, which are readily prepared by the reaction of ligand **2** with $[M(Ztpy)Cl_3]$ (M = Ru or Os; Z = H or thienyl) under reducing conditions (Scheme 1). As representative compounds, we describe herein complexes with tpy and 4′-(2-thienyl)-2,2′:6′,2″-terpyridine (**5**) auxiliary ligands decorating the surface (ligands as depicted in Scheme 2). The choice of **5** arose from the unusual chemical and photophysical properties of complexes with this ligand.[16,19] All new complexes were fully characterised and exhibited the expected spectroscopic properties. ^{1}H NMR spectroscopy is particularly useful for the characterisation of these complexes and the singlets due to the H3 protons of the central pyridine rings of the tpy domains make these useful spectator groups as the polynuclear systems are developed.

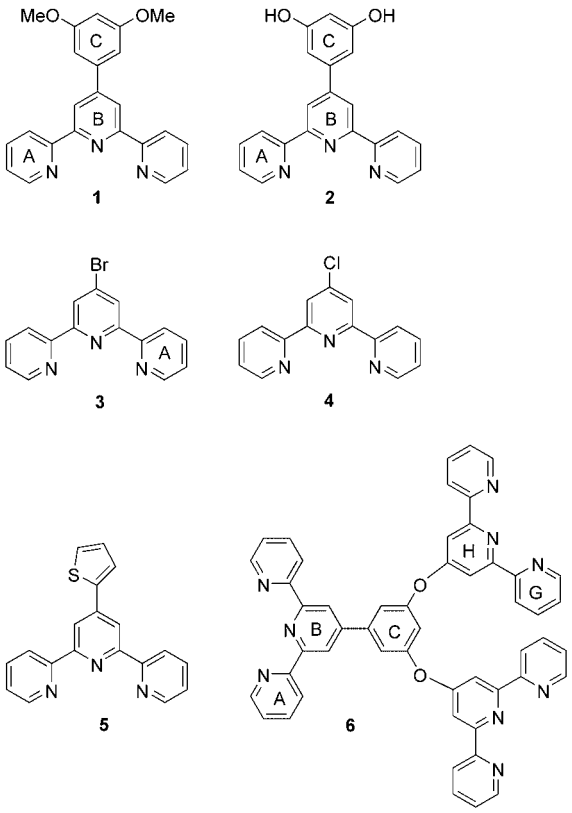

Scheme 2. Structures and ring-labelling scheme for the ligands.

Herein, we describe systems with up to 11 magnetically independent aromatic rings and make a note here of the nomenclature used. In ligand **2** and functionalised derivatives thereof, the terminal rings of the tpy are always denoted as A and the central tpy ring as B, with the phenyl substituent being the C ring. The constituent rings of the Ztpy ligand in $[M(Ztpy)(\mathbf{2})]^{2+}$ (Scheme 1) and derivatives are described as rings D (terminal), E (central) and F (thienyl substituent). For mononuclear complexes not containing **2**, A, B and C denote a tpy ligand ready for use in the metal-directed assembly step (usually 4′-chloro-2,2′:6′,2″-terpyridine **4** or 4′-bromo-2,2′:6′,2″-terpyridine **3**).

We have previously shown that complexes containing 4′-halopyridine moieties are activated towards attack at the C-4′ position by nucleophiles,[20,21] and we have used this phenomenon for the preparation of metallorods, metallostars and metallodendrimers[5,7,13] by reaction with oxygen-based nucleophiles. The complexes $[M(Ztpy)(\mathbf{2})]^{2+}$ (M = Ru or Os, Ztpy = tpy or **5**) react smoothly with the electrophilic complexes $[Ru(Ztpy)(Xtpy)]^{2+}$ (M = Ru or Os; Ztpy = tpy or **5**, Xtpy = **3** or **4**) in MeCN in the presence of K_2CO_3 to give the desired homo- or heterometallic trinuclear complexes $[(Ztpy)M(\mathbf{6})\{Ru(Ztpy)\}_2]^{6+}$ containing the new bifurcated tritopic bridging ligand **6** (Scheme 3).

The trinuclear complexes are V-shaped and intermetallic distances may be estimated by molecular modelling. We have modelled these complexes using molecular mechanics methods (MMFF in Spartan ′04), and although this approach ignores intercation repulsion, interactions within and between ligands are handled well. By constraining the metric quantities within the $\{M(tpy)_2\}$ units to crystallographically observed values ($M-N_{terminal}$ 2.07 Å; $M-N_{central}$ 1.98 Å), reliable structures may be obtained (Figure 1). In particular, we note that the chemically sensible and sterically favoured orientation of one {(Otpy)Ru(tpy)} motif above and the other below the phenyl ring reproduces well that found in the only structurally characterised noncyclic 3,5-diaryloxyarene.[22] The $M_{central}\cdots Ru_{outer}$ and $Ru_{outer}\cdots Ru_{outer}$ distances are in the ranges 12.3–12.6 Å and 14.0–14.2 Å, respectively. Spectroscopic and other properties will be discussed together with those of the pentanuclear species.

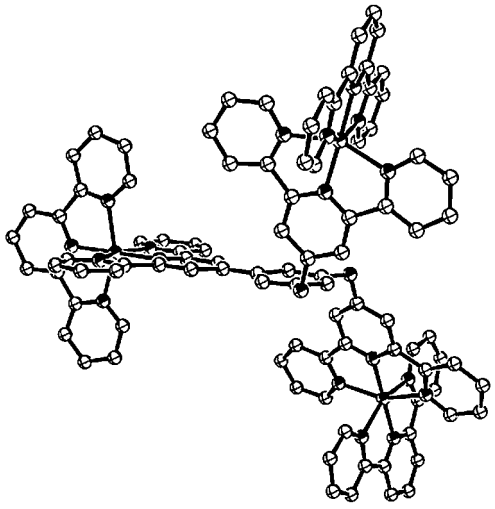

Figure 1. MMFF (Spartan ′04) minimised structure of the trinuclear V-shaped complex $[(tpy)Ru(\mathbf{6})\{Ru(tpy)\}_2]$ showing the expected conformation of the ether-linked moieties; the $Ru_{central}\cdots Ru_{outer}$ and $Ru_{outer}\cdots Ru_{outer}$ distances are in the ranges 12.3–12.6 Å and 14.0–14.2 Å, respectively. Hydrogen atoms have been omitted for clarity.

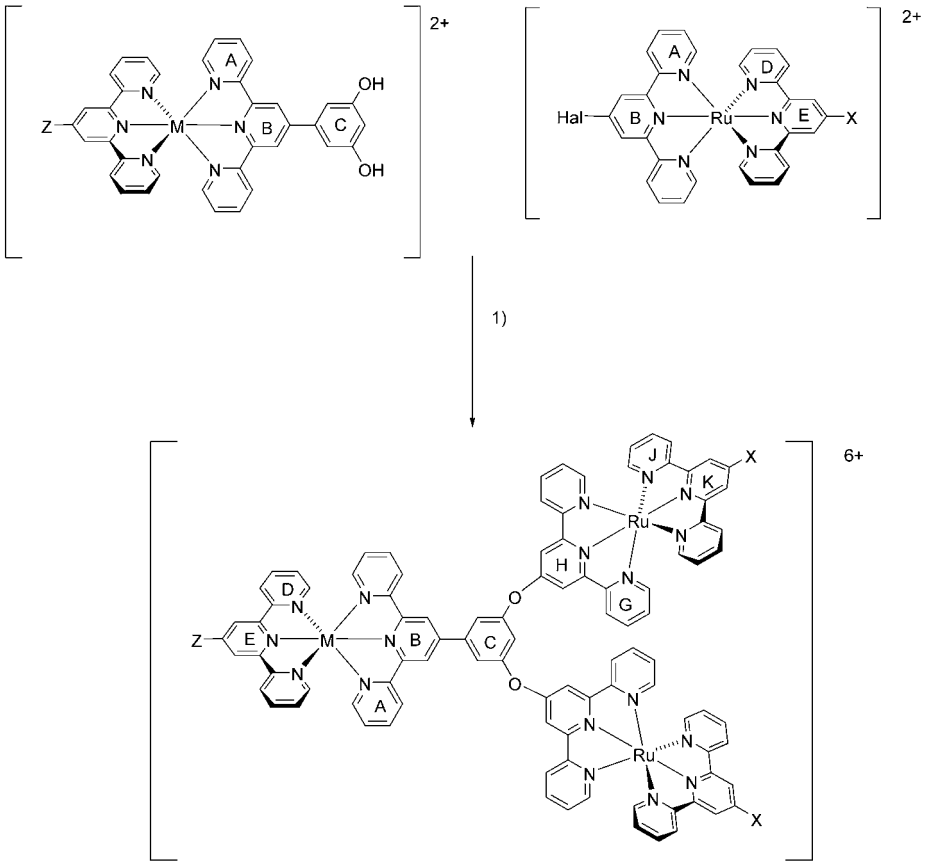

Scheme 3. Synthesis of the bifurcated trinuclear complexes showing the ring-labelling scheme adopted. 1) K_2CO_3, MeCN; M = Os or Ru, Z, X = H (tpy) or 2-thienyl (**5**). In the case of the complexes with **5**, the thienyl ring is labelled F when it is in the central position attached to ring E, but is labelled L when attached to the terminal sites on ring K.

Synthesis of the pentanuclear complexes: The same strategy as described above was adopted for the preparation of the X-shaped pentanuclear species, with the key intermediates being the tetraphenolic complexes $[M(\mathbf{2})_2]^{2+}$. Reaction of $[M(\mathbf{2})_2]^{2+}$ with $[M(Ztpy)(Xtpy)]^{2+}$ (M = Ru or Os; Ztpy = tpy or **5**, Xtpy = **3** or **4**) in MeCN in the presence of K_2CO_3 gave the homo- or heterometallic pentanuclear complexes $[M((\mathbf{6})\{Ru(Ztpy)\}_2)_2]^{10+}$ in moderate but acceptable yields (Scheme 4).

Characterisation of the complexes: The ^1H NMR spectra of all the trinuclear and pentanuclear complexes are sharp and well-resolved and have been fully assigned by a combination of NOESY and COSY techniques. Figure 2 shows the 500 MHz COSY 90 spectrum of a solution of the V-shaped complex $[(tpy)Ru(\mathbf{6})\{Ru(tpy)\}_2][PF_6]_6$ in CD_3CN, illustrating how all 24 pyridine proton environments are readily observed and how the connectivity within each of the magnetically independent subspectra may be established. The most noticeable feature on going from the complexes of **2** to those of **6** is a downfield shift of the signals of the C2 ($\delta = 7.11 \pm 0.02$ ppm) and C4 ($\delta = 6.55 \pm 0.04$ ppm) protons by 1.36 and 1.44 ppm, respectively. The other indicator peak for the coupling reaction is that due to proton B3, which shifts downfield from $\delta = 8.92 \pm 0.04$ ppm to $\delta = 9.35 \pm 0.07$ ppm.

The ES mass spectra of the complexes provide compelling evidence for the coupling reactions and the nuclearity of the products; in addition to the expected $[M-PF_6]^+$ peaks, series of peaks arising from more highly charged ions with the appropriate isotopomer distributions and peak separations are observed. For example, the ES mass spectrum of $[Ru((\mathbf{6})\{Ru(tpy)\}_2)_2][PF_6]_{10}$ exhibits clusters of peaks with m/z corresponding to $[M-2PF_6]^{2+}$, $[M-3PF_6]^{3+}$, $[M-4PF_6]^{4+}$, $[M-5PF_6]^{5+}$ and $[M-6PF_6]^{6+}$, all of which show the expected isotopomer distributions for pentaruthenium species.

Electrochemical properties of the complexes: All of the metal complexes are redox-active, showing both metal-centred and ligand-centred processes (Table 1). Those complexes

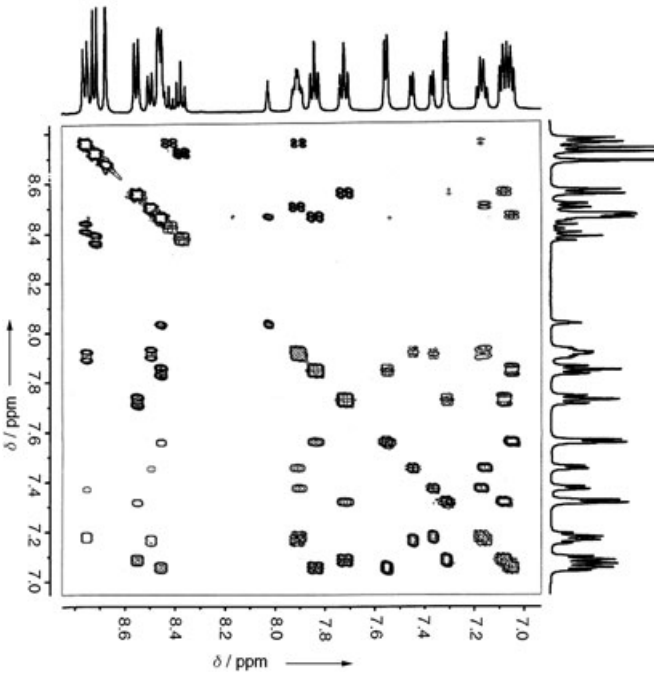

Figure 2. 500 MHz COSY 90 spectrum (room temperature) of a solution of $[(tpy)Ru(\mathbf{6})\{Ru(tpy)\}_2][PF_6]_6$ in CD_3CN.

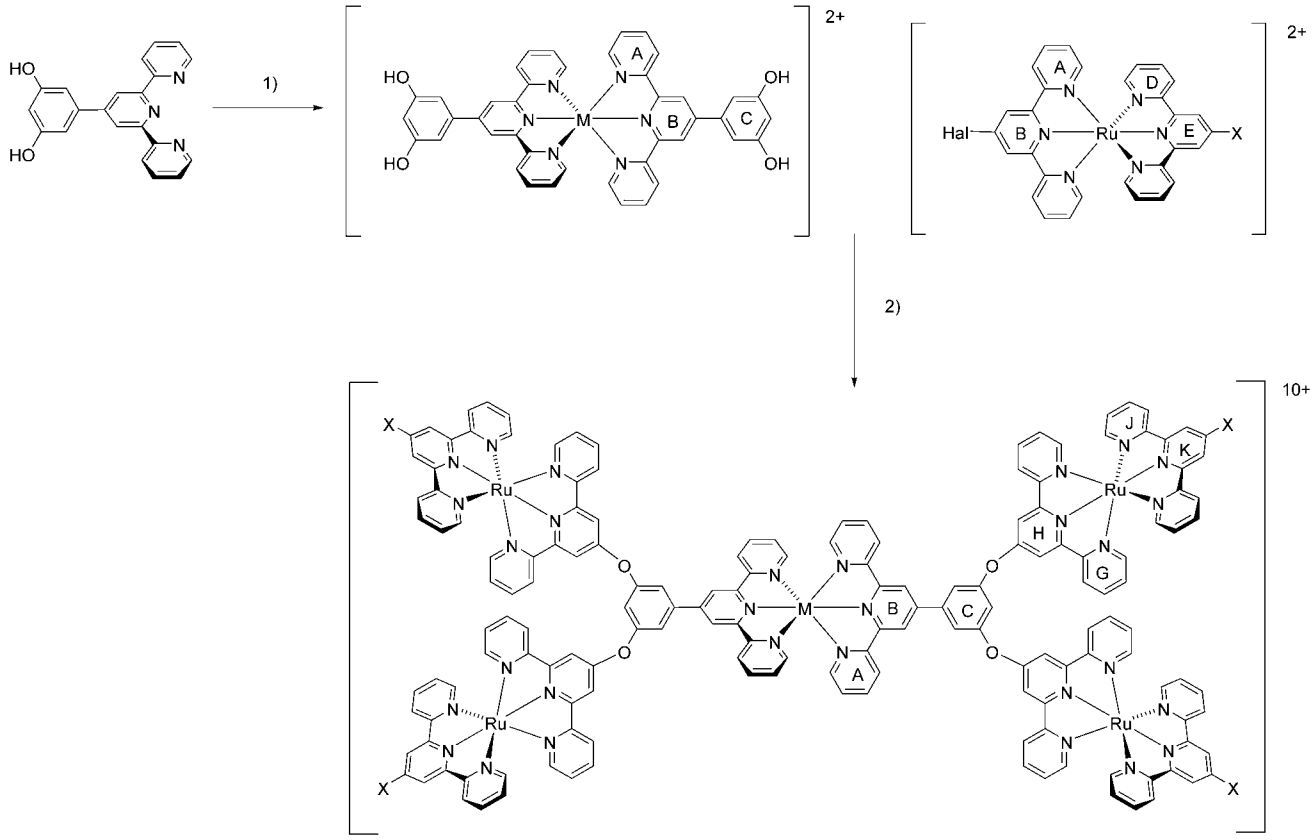

Scheme 4. Synthesis of the dendritic pentanuclear complexes showing the ring-labelling scheme adopted. 1) $RuCl_3 \cdot 3H_2O$ or $K_2[OsCl_6]$, ethane-1,2-diol, *N*-ethylmorpholine, microwave; 2) K_2CO_3, MeCN; M = Os or Ru, X = H (tpy) or 2-thienyl (**5**). In the case of the complexes with **5**, the thienyl ring is labelled L.

Table 1. Redox potentials (E ($E_a - E_c$) in volts) measured by cyclic or square-wave voltammetry of the mononuclear building blocks and metallostars in MeCN (1.0 M $[n\mathrm{Bu_4N}][\mathrm{PF_6}]$, Pt or glassy carbon working electrode, Pt wire counter-electrode, Ag wire, referenced against internal Fc/Fc^+). All metal-based processes were reversible;[a] the ligand reductions were irreversible and potentials are taken from the forward scan. All complexes were used as hexafluorophosphate salts.

Compound	Ligand	Ru	Os	tpy
$[(tpy)Ru(\mathbf{3})]^{2+}$		0.920		−1.55, −1.67, −1.93
$[(\mathbf{5})Ru(\mathbf{4})]^{2+}$		0.896		−1.56, −1.80
$[(tpy)Ru(\mathbf{2})]^{2+}$	1.34	0.901		−1.64, −1.85
$[(\mathbf{5})Ru(\mathbf{2})]^{2+}$	1.77	0.889		−1.27, −1.72, −1.94
$[(\mathbf{5})Os(\mathbf{2})]^{2+}$	1.78, 1.56		0.535	−1.56, −1.79
$[Os\{\mathbf{2}\}_2]^{2+}$			0.516	−1.38, −1.66
$[(tpy)Ru(\mathbf{6})\{Ru(tpy)\}_2]^{6+}$		0.854		−1.62, −1.83, −1.99
$[(\mathbf{5})Ru(\mathbf{6})\{Ru(tpy)\}_2]^{6+}$	1.72	0.846		−1.60, −1.80, −1.93
$[(\mathbf{5})Os(\mathbf{6})\{Ru(tpy)\}_2]^{6+}$	1.45	0.840	0.535	−1.62, −1.77, −1.95
$[(\mathbf{5})Os(\mathbf{6})\{Ru(\mathbf{5})\}_2]^{6+}$	1.47	0.824	0.543	−1.60, −1.79, −1.98
$[Ru((\mathbf{6})\{Ru(tpy)\}_2)_2]^{10+}$		0.892		−1.63, −1.81
$[Os((\mathbf{6})\{Ru(\mathbf{5})\}_2)_2]^{10+}$	1.48	0.835	0.563	−1.61, −1.78, −1.95

[a] Reversible peaks showed the same $\Delta E = E_a - E_c$ as ferrocene in the same solvent.

containing ligand **5** also exhibit thiophene-based oxidation waves. In acetonitrile solution, the ruthenium and osmium complexes exhibit reversible metal(III)/metal(II) processes at +0.8 to +0.9 and +0.5 to +0.6 V (versus Fc/Fc^+), respectively, typical of the $\{M(tpy)_2\}$ centres present. It was not possible to resolve separate metal-centred processes corresponding to the central and the outer metals for the triruthenium and pentaruthenium processes by cyclic voltammetry, differential pulse voltammetry or square-wave voltammetry, and a single, apparently reversible wave was observed. However, in the heterometallic complexes $[(\mathbf{5})Os(\mathbf{6})\{Ru(tpy)\}_2][PF_6]_6$, $[(\mathbf{5})Os(\mathbf{6})\{Ru(\mathbf{5})\}_2][PF_6]_6$ and $[Os((\mathbf{6})\{Ru(\mathbf{5})\}_2)_2][PF_6]_{10}$, both osmium and ruthenium processes in the correct current ratio are observed, indicating that the observation of a single signal for the tri- and pentaruthenium complexes arises from an unfortunate degeneracy of the redox processes for the inner and outer centres, rather than a shifting of one of the two processes out of the observable window subsequent to the oxidation of either the inner or outer metal centres.

Absorption and emission spectroscopy: Table 2 lists absorption maxima and absorption coefficients for solutions of the tri- and pentanuclear complexes in MeCN as well as those

Table 2. Absorption spectroscopic data for the polynuclear complexes and related mononuclear building blocks. All data are for solutions of $[PF_6]^-$ salts in MeCN at room temperature.

Compound	MLCT λ_{max} [nm] (ε_{max} [10^4 dm^{3}mol^{-1}cm^{-1}])	Ligand centred λ_{max} [nm] (ε_{max} [10^4 dm^{3}mol^{-1}cm^{-1}])
$[(tpy)Ru(\mathbf{3})]^{2+}$	480 (1.5)	324 sh, 307 (5.9), 272 (4.0)
$[(\mathbf{5})Ru(\mathbf{4})]^{2+}$	490 (2.6)	326 sh, 305 (6.3), 275 (4.6)
$[(tpy)Ru(\mathbf{2})]^{2+}$	480 (1.7)	330 sh, 306 (5.6), 272 (3.8)
$[(\mathbf{5})Ru(\mathbf{2})]^{2+}$	495 (2.1)	330 sh, 311 (4.9), 283 (4.4)
$[(\mathbf{5})Os(\mathbf{2})]^{2+}$	670 (0.78), 494 (2.9)	314 (2.24), 284 (5.7)
$[Ru(\mathbf{2})_2]^{2+}$	490 (2.0)	329 sh, 310 (5.1), 284 (4.3)
$[Os(\mathbf{2})_2]^{2+}$	670 (0.50), 489 (2.0)	331 sh, 314 (6.0), 285 (5.0)
$[(tpy)Ru(\mathbf{6})\{Ru(tpy)\}_2]^{6+}$	480 (5.0)	324 sh, 306 (16.0), 272 (12.0)
$[(\mathbf{5})Ru(\mathbf{6})\{Ru(tpy)\}_2]^{6+}$	490 (4.8)	329 sh, 306 (13.5), 275 (10.7)
$[(\mathbf{5})Os(\mathbf{6})\{Ru(tpy)\}_2]^{6+}$	670 (0.8), 490 (6.0)	306 (17.0), 276 (13.0)
$[(\mathbf{5})Os(\mathbf{6})\{Ru(\mathbf{5})\}_2]^{6+}$	670 (0.8), 500 (7.0)	330 sh, 306 (18.0), 285 (16.0)
$[Ru((\mathbf{6})\{Ru(tpy)\}_2)_2]^{10+}$	485 (10.5)	306 (26.0), 275 (24.0)
$[Os((\mathbf{6})\{Ru(\mathbf{5})\}_2)_2]^{10+}$	670 (0.71), 495 (10.5)	331 sh, 306 (22.0), 286 (19.0)

for the relevant mononuclear building blocks. All of the complexes exhibit intense UV absorption bands corresponding to ligand-centred (^{1}LC) transitions, and absorptions in the visible region attributable to metal-to-ligand charge-transfer (^{1}MLCT) transitions. These latter bands fall in the range 480–490 nm (with absorption coefficients $\varepsilon = 1.4$–2.6×10^4 M^{-1} cm^{-1} per {M(tpy)$_2$} chromophore for both Ru^{II} and Os^{II} centres). An additional absorption at $\approx$670 nm ($\varepsilon = (6 \pm 2) \times 10^3$ M^{-1} cm^{-1}) is observed for the Os^{II}-containing complexes and is assigned to the formally spin-forbidden transition directly to the {Os(tpy)$_2$} ^{3}MLCT state.[23] Table 3 lists the luminescence properties of model mononuclear complexes along with those of the new trinuclear and pentanuclear complexes, as observed at room temperature and at 77 K in air-equilibrated acetonitrile.

The spectroscopic properties of the trinuclear complexes $[(\mathbf{5})Os(\mathbf{6})\{Ru(tpy)\}_2]^{6+}$ and $[(\mathbf{5})Os(\mathbf{6})\{Ru(\mathbf{5})\}_2]^{6+}$ have been briefly discussed in a previous report.[9] The pendant thienyl group was found to stabilise (redshift) the MLCT levels involving ligand **5**, for both the absorption and emission features. This resulted in a modulation of the Ru→Os energy transfer rate between $[(\mathbf{5})Os(\mathbf{6})\{Ru(\mathbf{5})\}_2]^{6+}$ and $[(\mathbf{5})Os(\mathbf{6})\{Ru(tpy)\}_2]^{6+}$. In points 1)–4) below, we describe the results obtained at room temperature. The glassy matrix data at 77 K are discussed later.

1) Each member of the series of V-shaped trinuclear and X-shaped pentanuclear complexes can be considered in terms of clearly defined building blocks. This is evident from the absorption spectra of the polynuclear species, which appear as superimpositions of the spectra of the component mononuclear model complexes. This is consistent with a substantial ground-state electronic decoupling of the components, as a consequence of the insulating character of the ether connections.[9,11] Similar conclusions follow from the electrochemical data (Table 1). With regard to the pentanuclear species, the absorption spectra presented in Figure 3 provide an illustration of this point, with the additional consideration that the presence of the thienyl group in ligand **5** stabilises the MLCT levels involving this ligand.

2) The mononuclear and homometallic polynuclear complexes of ruthenium(II) are all very weak emitters at room temperature ($\Phi < 10^{-4}$, $\lambda_{max} = 630$–670 nm, $\lambda_{exc} = 480$ nm), with lifetimes in the range of few nanoseconds or less (Table 3). These features are in general agreement with the wealth of results from other complexes based on {Ru(tpy)$_2$} chromophores.[23]

Table 3. Luminescence properties of model mononuclear complexes and those of the new trinuclear and pentanuclear complexes.[a]

	298 K						77 K			
	Ru-based region			Os-based region			Ru-based region		Os-based region	
	λ_{max} [nm]	$10^5\,\phi$	τ [ns]	λ_{max} [nm]	$10^2\,\phi$	τ [ns]	λ_{max} [nm]	τ [μs]	λ_{max} [nm]	τ [μs]
$[(tpy)Ru(\mathbf{2})]^{2+}$[b]	630	<3.0	0.6				615	11.0		
$[Ru(\mathbf{2})_2]^{2+}$	634	4.5	1.4				622	10.5		
$[(\mathbf{5})Ru(\mathbf{2})]^{2+}$[b]	670	15.0	6.4				654	11.5		
$[Os(\mathbf{2})_2]^{2+}$				732	1.8	110			722	2.0
$[(\mathbf{5})Os(\mathbf{2})]^{2+}$[b]				744	2.0	150			745	2.0
$[(tpy)Ru(\mathbf{6})\{Ru(tpy)\}_2]^{6+}$	640	<3.0	≤0.6				630	11.0		
$[(\mathbf{5})Ru(\mathbf{6})\{Ru(tpy)\}_2]^{6+}$	670	<3.0	≤0.6				650	10.0		
$[(\mathbf{5})Os(\mathbf{6})\{Ru(tpy)\}_2]^{6+}$[b]	[c]	[c]	[c]	745	(0.6)	120	630	1.8×10^{-3}	750	1.6×10^{-3}[d] 2.0[d]
$[(\mathbf{5})Os(\mathbf{6})\{Ru(\mathbf{5})\}_2]^{6+}$[b]	[c]	[c]	[c]	745	(0.5)	120	630	$>5 \times 10^{-3}$[b]	750	36.0×10^{-3}[d] 2.0[d]
$[Ru((\mathbf{6})\{Ru(tpy)\}_2)_2]^{10+}$	662	3.6	~1				630	10.3		
$[Os((\mathbf{6})\{Ru(\mathbf{5})\}_2)_2]^{10+}$	[c]	[c]	[c]	740	0.5	110	656	34×10^{-3}	724	39×10^{-3}[d] 2.0[d]

[a] In air-equilibrated acetonitrile solvent, $\lambda_{exc} = 480$ nm; $[(tpy)Ru(\mathbf{3})]^{2+}$ and $[(\mathbf{5})Ru(\mathbf{4})]^{2+}$ are both very weak emitters at room temperature, $\phi < 3 \times 10^{-5}$, and have not been investigated in detail. [b] See also ref. [9]. [c] Too weak to detect. [d] Dual exponential behaviour; the indicated values refer to τ_1 and τ_2 of $I(t) = b_1 \exp(-t/\tau_1) + b_2 \exp(-t/\tau_2)$, where b_1 and b_2 are pre-exponential factors, and b_1 is a negative value (see text).

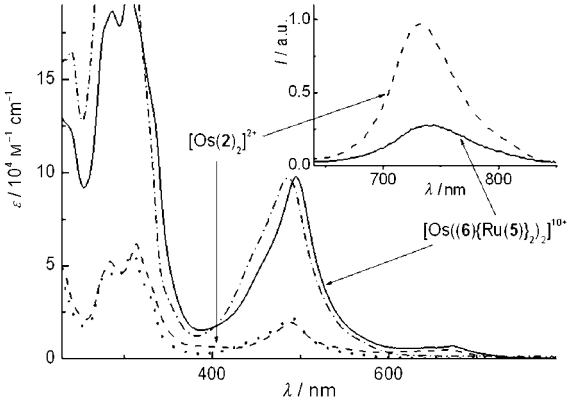

Figure 3. The ground-state absorption spectra of $[Os((\mathbf{6})\{Ru(\mathbf{5})\}_2)_2]^{10+}$ (——), $[Os(\mathbf{2})_2]^{2+}$ (– – –), $[Ru(\mathbf{2})(\mathbf{5})]^{2+}$ (•••••) and $[Ru((\mathbf{6})\{Ru(tpy)\}_2)_2]^{10+}$ (–•–•). The inset shows the room temperature luminescence spectra of $[Os((\mathbf{6})\{Ru(\mathbf{5})\}_2)_2]^{10+}$ (——) and $[Os(\mathbf{2})_2]^{2+}$ (– – –), as obtained from isoabsorbing solutions at $\lambda_{exc}=480$ nm.

3) The mononuclear osmium(II) complexes, $[Os(\mathbf{2})_2]^{2+}$ and $[(\mathbf{5})Os(\mathbf{2})]^{2+}$, are more strongly emitting than their ruthenium(II) analogues and exhibit luminescence quantum yields $\Phi \sim 2\times10^{-3}$ ($\lambda_{max}=732$ and 744 nm, respectively, $\lambda_{exc}=$ 480 nm) with luminescence lifetimes of 110 and 150 ns, respectively. These wavelengths and lifetime features are typical, and indeed characteristic, of $\{Os(tpy)_2\}$ luminophores in fluid solution at room temperature.[23]

4) For the heterometallic species $[(\mathbf{5})Os(\mathbf{6})\{Ru(tpy)\}_2]^{6+}$, $[(\mathbf{5})Os(\mathbf{6})\{Ru(\mathbf{5})\}_2]^{6+}$ and $[Os((\mathbf{6})\{Ru(tpy)\}_2)_2]^{10+}$, excitation at room temperature at 480 nm (at which both Ru-based and Os-based chromophores are isoabsorptive and absorb light in approximately 2:1 and 4:1 ratios for the trinuclear and pentanuclear species, respectively), no ruthenium-based emission (below 700 nm) is detected. Instead, only osmium-based emissions at greater than 700 nm are observed for these heterometallic complexes. This conclusion is based on a comparison of the λ_{max} and τ values listed in Table 3. In addition, for the heterometallic species, the luminescence yield is $\phi=0.5$–0.6×10^{-2}, that is, a third to a quarter of that of the reference mononuclear complexes $[Os(\mathbf{2})_2]^{2+}$ and $[(\mathbf{5})Os(\mathbf{2})]^{2+}$. This can be rationalised by the fact that, in the heterometallic complexes at room temperature, the fraction of light absorbed by the ruthenium-based chromophores does not result in Ru→Os energy transfer (which is energetically allowed, with the osmium states lying ~0.25 eV lower in energy, as estimated from the ruthenium- and osmium-based emission band maxima (Table 3)) and no sensitisation of the $\{Os(tpy)_2\}$ luminescence occurs. On this basis, and given that the lifetimes of the ruthenium-based luminophores investigated here are in the range 0.6 to 6 ns (at room temperature, see Table 3), one concludes that the Ru→Os intramolecular energy transfer must be slower than the intrinsic deactivation, $k_{en}\leq k_d$, with $k_d=1.6$–$10\times10^8\ s^{-1}$. Conversely, only the fraction of light directly absorbed by the osmium-based chromophores is responsible for the observed osmium-based luminescence intensities. This is illustrated by the inset in Figure 3, which displays the room temperature luminescence spectra obtained by excitation of isoabsorbing (480 nm) solutions of $[Os(\mathbf{2})_2]^{2+}$ and $[Os((\mathbf{6})\{Ru(\mathbf{5})\}_2)_2]^{10+}$, the luminescence intensities of which are in an approximate 4:1 ratio. We stress the fact that upon 480 nm excitation of isoabsorbing solutions followed by hypothetical *complete* Ru→Os energy transfer, identical Os-based luminescence intensities would be expected for $[Os(\mathbf{2})_2]^{2+}$ and $[Os((\mathbf{6})\{Ru(\mathbf{5})\}_2)_2]^{10+}$.[24,25]

With regard to measurements at 77 K in frozen solvent, Figure 4 shows the normalised luminescence profiles of the pentanuclear complex $[Os((\mathbf{6})\{Ru(\mathbf{5})\}_2)_2]^{10+}$, along with

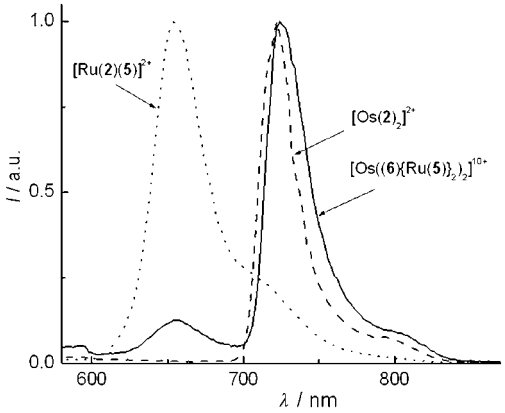

Figure 4. Normalised luminescence spectra at 77 K for $[Os((\mathbf{6})\{Ru(\mathbf{5})\}_2)_2]^{10+}$ (——), $[Os(\mathbf{2})_2]^{2+}$ (– – –) and $[Ru(\mathbf{2})(\mathbf{5})]^{2+}$ (•••••); $\lambda_{exc}=480$ nm in all cases.

those of $[(\mathbf{5})Ru(\mathbf{2})]^{2+}$ and $[Os(\mathbf{2})_2]^{2+}$, the mononuclear complexes that can be regarded as the reference component units. It can be seen that for the pentanuclear complex, the ruthenium-based emission region at 650 nm exhibits a strong reduction in intensity compared to the mononuclear reference compound. Evidence for quenching and sensitisation phenomena can be gained from time-resolved experiments, as illustrated for $[Os((\mathbf{6})\{Ru(\mathbf{5})\}_2)_2]^{10+}$ in Figure 5. In particular, while the luminescence of $[(\mathbf{5})Ru(\mathbf{2})]^{2+}$ (observed at 650 nm) is rather long-lived ($\tau=11.5$ μs), the Ru-based emission for $[Os((\mathbf{6})\{Ru(\mathbf{5})\}_2)_2]^{10+}$ (observed at 650 nm) exhibits $\tau^{Ru}=34$ ns. In addition, for this complex, the analysis of the luminescence decay detected at 730 nm (osmium-based emission region) required a dual exponential law, $I(t)=b_1\exp(-t/\tau_1)+b_2\exp(-t/\tau_2)$, where b_1 and b_2 are pre-exponential factors, and b_1 is a negative value. In this case, we found $\tau_1=39$ ns and $\tau_2=2.0$ μs. Further results relating to the time-dependent luminescence properties of the complexes are collected in Table 3.

Photoinduced processes: The results obtained at 77 K (Figures 4 and 5) are consistent with effective intramolecular Ru→Os energy transfer in $[Os((\mathbf{6})\{Ru(\mathbf{5})\}_2)_2]^{10+}$. This causes quenching of the donor luminescence ($\tau_q^{Ru}=34$ ns, as op-

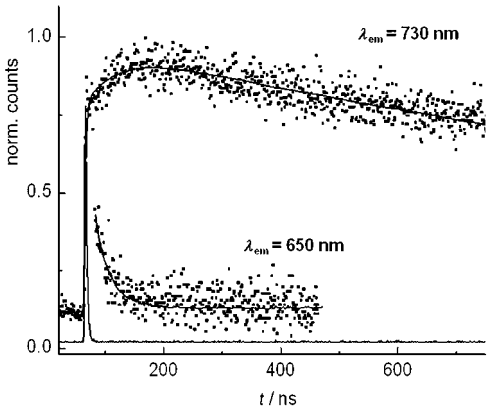

Figure 5. Time-resolved luminescence properties of $[Os((\mathbf{6})\{Ru(\mathbf{5})\}_2)_2]^{10+}$ at 77 K, as observed at 650 nm (ruthenium-based region, single-exponential decay, $\tau = 34$ ns) and 730 nm (osmium-based region, dual-exponential decay, $\tau_1 = 39$ ns and $\tau_2 = 2.0$ μs); see text and Table 3. The time profile of the 465 nm NanoLED excitation source is also shown (norm. = normalised.).

posed to $\tau^{Ru} = 11.5$ μs in the reference complex $[(\mathbf{5})Ru(\mathbf{2})]^{2+}$), and concomitant sensitisation of the osmium-based luminescence with $\tau_1 = 39$ ns (a rise time, see Figure 5) and $\tau_2 = 2.0$ μs. The Ru→Os energy-transfer rate constant k_{en} can then be calculated according to $k_{en} = 1/\tau_q^{Ru} - 1/\tau^{Ru}$. This yields $k_{en} = 2.6 \times 10^7\ s^{-1}$, practically identical to the value found previously for the trinuclear complex $[(\mathbf{5})Os(\mathbf{6})\{Ru(\mathbf{5})\}_2]^{6+}$, $k_{en} = 2.8 \times 10^7\ s^{-1}$.[9] This is consistent with an energy-transfer efficiency, $\phi_{en} \sim$ unity, defined in Equation (1):

$$\phi_{en} = \frac{k_{en}}{k_{en} + k_d} \tag{1}$$

in which k_d is the intrinsic deactivation rate constant for the unquenched Ru-based donor determined for the model; $k_d = 1/\tau^{Ru}$, with $\tau^{Ru} = 11.5$ μs (Table 3). Given the insulating character of the ether linkage,[9,11] the Ru→Os energy-transfer step within the trinuclear and pentanuclear species can be described using the Förster dipole–dipole energy-transfer approach[12,26] [Eqs. (2a)–(2c)]:

$$J_F = \frac{\int F(\tilde{\nu})\varepsilon(\tilde{\nu})/\tilde{\nu}^4 d\tilde{\nu}}{\int F(\tilde{\nu})} \tag{2a}$$

$$R_0 = 9.79 \times 10^3 (K^2 \eta^{-4} \Phi J_F)^{1/6} \tag{2b}$$

$$k_{en} = k_d \left(\frac{R_0}{d_{cc}}\right)^6 \tag{2c}$$

Here, J_F is the Förster overlap integral between the luminescence spectrum of the donor, $F(\tilde{\nu})$, and the absorption spectrum of the acceptor, $\varepsilon(\tilde{\nu})$, on an energy scale (cm^{-1}); R_0 is the critical transfer radius (the interchromophore distance for which the energy-transfer efficiency is $\phi_{en} = 0.5$); K^2 is a geometric factor (for statistical reasons, $K^2 = {}^2/_3$), ϕ and τ are the luminescence quantum yield and lifetime of the donor, respectively; η is the refractive index of the solvent and d_{cc} is the interchromophore distance. By using the 77 K luminescence properties of the donor model complex $[(\mathbf{5})Ru(\mathbf{2})]^{2+}$, $\tau = 11.5$ μs and $\phi = 0.30$,[9] and the absorption features of the acceptor model $[Os(\mathbf{2})_2]^{2+}$, for the pentanuclear case one obtains $J_F = 6.7 \times 10^{-14}\ cm^3\,M^{-1}$ and $R_0 = 39$ Å. Based on Equation (2c), $d_{cc} = 15$ Å (cf. 16.5 Å for $[(\mathbf{5})Os(\mathbf{6})\{Ru(\mathbf{5})\}_2]^{6+}$[9]), consistent with the molecular-modelling results.

In summary, for the heterometallic trinuclear and pentanuclear species at 77 K (Table 3), the Ru→Os energy transfer is quite an efficient process, at variance with what is observed at room temperature. This can be understood on the basis of the fact that Ru→Os energy transfer for tpy-type complexes is little affected by the temperature or the state (fluid or frozen) of the solvent.[27] Thus, at room temperature, the intrinsic deactivation at the Ru-based donor unit (Table 3) is much faster than energy transfer, $k_d^{RT} > k_{en}$; the reverse is true at 77 K, $k_d^{77K} < k_{en}$.

Conclusion

We have demonstrated that the use of metal-activated organic electrophiles is an efficient and controllable method for the preparation of V-shaped metallorods and X-shaped metallostars. In particular, $[(\mathbf{5})Os(\mathbf{6})\{Ru(tpy)\}_2]^{6+}$ and $[Os((\mathbf{6})\{Ru(\mathbf{5})\}_2)_2]^{10+}$ are of special interest as the ruthenium-to-osmium energy transfer is temperature dependent. At low temperatures, the energy transfer is efficient and osmium-centred emission is observed, whereas at room temperature the ruthenium luminophores are efficiently deactivated and no energy transfer is observed. These observations introduce an additional parameter that may be adjusted in order to tune the energy-transfer processes in antenna devices.

Experimental Section

General methods: Infrared spectra were recorded on Mattson Genesis and Shimadzu FTIR 8300 Fourier-transform spectrophotometers with samples in compressed KBr discs or as solids using a Golden Gate ATR accessory. ^1H and ^{13}C NMR spectra were recorded on Bruker AC 300, AV 300 and DRX 500 spectrometers at room temperature; the ring-labelling scheme adopted for the ligands is shown in the structure diagrams; chemical shifts are referenced with respect to TMS ($\delta = 0$ ppm). EI mass spectra were recorded on a Kratos MS 50 instrument. Electrospray mass spectra (ES-MS) were recorded by using Finnigan MAT LCT and LCQ mass spectrometers. Electrochemical measurements were performed with an Autolab PGSTAT 20 system using platinum or glassy-carbon working and auxiliary electrodes with an Ag/AgCl electrode as reference, using purified acetonitrile as solvent and 0.1 M $[n Bu_4N][BF_4]$ as the supporting electrolyte. Potentials are quoted versus the ferrocene/ferrocenium couple ($Fc/Fc^+ = 0.0$ V) and were referenced to internal ferrocene added at the end of each experiment. All glassware was flame-dried prior to use and flushed with N_2; K_2CO_3 was dried at 170 °C for at least 24 h before use.

Absorption spectra of dilute solutions in acetonitrile ($1–2\times10^{-5}$ M) were measured with a Perkin-Elmer Lambda 45 UV/Vis spectrophotometer. Luminescence spectra were obtained with a Spex Fluorolog II spectrofluorimeter equipped with a Hamamatsu R928 phototube. Air-equilibrated sample solutions were excited at 480 nm and their concentrations were adjusted so as to obtain absorbance values ≤ 0.15. Low-temperature measurements were performed using capillary tubes immersed in liquid nitrogen. Whilst uncorrected luminescence band maxima are referred to throughout the text, corrected spectra were employed for the determination of the luminescence quantum yields (the correction procedure was based on the use of software that takes care of the wavelength-dependent phototube response). From the wavelength-integrated area of the corrected luminescence spectra, we obtained luminescence quantum yields ϕ for the samples with reference to $[Ru(bpy)_3]Cl_2$ (r, $\phi_r = 0.028$ in air-equilibrated water[28]) through the use of Equation (3):[29]

$$\frac{\phi}{\phi_r} = \frac{A_r \eta^2(\text{area})}{A \eta_r^2(\text{area})_r} \quad (3)$$

in which A and η refer to the absorbance values and refractive indices of the two solutions. Band maxima and relative luminescence intensities were measured with estimated uncertainties of 2 nm and 20%, respectively. Luminescence lifetimes were measured using an IBH 5000F single-photon counting spectrometer; excitation was performed at 465 nm (with a NanoLED source); single- or double-exponential analyses of the decays were performed with the help of software provided by IBH. The estimated uncertainty for the lifetime values is 8%.

All metal complexes were repeatedly recrystallised prior to use in photophysical studies and were judged to be pure on the basis of chromatographic and spectroscopic studies. In our hands, combustion microanalyses of multinuclear ruthenium or ruthenium/osmium oligopyridine complexes have been found to result in data with anomalously low carbon figures due to carbide formation.

4′-(3,5-Dimethoxyphenyl)-2,2′:6′,2″-terpyridine (1): 2-Acetylpyridine (690 μL, 5.8 mmol) was added dropwise to a solution of KO*t*Bu (1.04 g, 9.3 mmol) in THF (50 mL) and the mixture was stirred at room temperature for 30 min to give a pale yellow suspension containing the enolate. A solution of 3,5-dimethoxybenzaldehyde (508 mg, 3.06 mmol) in THF (5 mL) was then added, whereupon the reaction mixture immediately became clear and bright orange. After stirring for 17 h at room temperature, a suspension of dried NH_4OAc (5 g) in 2:1 EtOH/AcOH (60 mL) was added and the reaction mixture was heated to reflux for 5 h. It was then cooled to room temperature, poured onto ice and after 2 h water (300 mL) was added, resulting in the deposition of **1** as an off-white precipitate, which was collected by filtration. Extraction of the filtrate with CH_2Cl_2 (100 mL) gave a brown oil from which a further small amount of **1** was obtained after chromatographic separation (Al_2O_3, toluene/5% Et_2NH). Yield: 545 mg (50.9%); ^{1}H NMR (300 MHz, $CDCl_3$): $\delta = 8.73$ (d, $J = 4.8$ Hz, 2H; A6), 8.69 (s, 2H; B3), 8.67 (d, $J = 8.1$ Hz, 2H; A3), 7.88 (dt, $J = 1.8$, 7.7 Hz, 2H; A4), 7.36 (ddd, 2H; A5), 7.01 (d, $J = 2.2$ Hz, 2H; C2), 6.56 (t, 1H; C4), 3.69 ppm (s, 6H; OCH_3); ^{13}C NMR (125 MHz, $CDCl_3$): $\delta = 161$ (C3), 156 (B2), 155 (A2), 150 (B4), 149 (A6), 140 (C1), 136 (A4), 123 (A5), 121 (A3), 119 (B3), 105 (C2), 101 (C4), 55 ppm (CH_3); IR (solid): $\tilde{\nu} = 2939$ (w), 2839 (w), 2360 (w), 1581 (s), 1465 (m), 1388 (s), 1334 (w), 1296 (w), 1203 (s), 1149 (s), 1064 (m), 987 (w), 894 (w), 786 (s), 732 (s), 694 (m), 655 cm^{-1} (s); MS (EI): m/z: 369 $[M]^+$, 339 $[M-2\text{Me}]^+$.

4′-(3,5-Dihydroxyphenyl)-2,2′:6′,2″-terpyridine (2): Concentrated hydrochloric acid (17.6 mL) and pyridine (16 mL) were heated under N_2 at 210°C for approximately 2 h with continuous removal of water until the solution reached a constant internal temperature of 210°C. After cooling to 150°C, **1** (1.1 g, 3.0 mmol) was added and the mixture was heated at 210°C for 3 h. It was then cooled to 100°C, whereupon warm water (60 mL) was added. The pale precipitate that formed was collected by filtration and dried over P_2O_5 in vacuo. Yield: quantitative; ^{1}H NMR (300 MHz, [D$_6$]DMSO): $\delta = 8.92$ (d, $J = 8.1$ Hz, 2H; A3), 8.86 (d, $J = 4.8$ Hz, 2H; A6), 8.73 (s, 2H; B3), 8.30 (dt, $J = 1.5$, 7.7 Hz, 2H; A4), 7.75 (dt, 2H; A5), 6.84 (d, $J = 2.2$ Hz, 2H; C2), 6.41 ppm (t, 1H; C4); ^{13}C NMR (100 MHz, [D$_6$]DMSO): $\delta = 147.4$ (A6), 140.1 (A4), 125.4 (A5), 122.2 (A3), 118.9 (B3), 104.8 (C2), 103.8 ppm (C4); due to low solubility, the quaternary C could not be observed; IR (solid): $\tilde{\nu} = 3055$ (m), 2827 (m), 2727 (m), 1593 (s), 1523 (s), 1473 (w), 1419 (m), 1353 (m), 1330 (m), 1292 (m), 1234 (m), 1215 (m), 1153 (s), 1095 (w), 1026 (m), 1002 (m), 956 (m), 879 (w), 844 (s), 783 (s), 729 (m), 702 (m), 678 (m), 648 (m), 617 (m), 567 (s), 532 cm^{-1} (m); MS (ESI, high resolution): m/z calcd for $C_{21}H_{16}N_3O_2$ $[M+H]^+$: 342.124; found: 342.123; MS (ESI): m/z: 364 $[M+\text{Na}]^+$, 342 $[M+\text{H}]^+$.

[Ru(tpy)(3)][PF$_6$]$_2$: A mixture of 4′-bromo-2,2′:6′,2″-terpyridine (**3**; 65.0 mg, 0.209 mmol), [Ru(tpy)Cl$_3$] (95.0 mg, 0.216 mmol) and *N*-ethylmorpholine (4 drops) in EtOH (20 mL) was heated at reflux for 3 h. Aqueous NH_4PF_6 was then added and the red precipitate that formed was collected by filtration. Purification of the crude product by column chromatography (SiO_2; MeCN/saturated aqueous KNO_3/H_2O, 7:1:0.5) gave [Ru(tpy)(**3**)][PF$_6$]$_2$ as an orange solid. Yield: 142 mg (72.5%); ^{1}H NMR (300 MHz, CD_3CN): $\delta = 8.97$ (s, 2H; B3), 8.73 (d, $J = 8.1$ Hz, 2H; E3), 8.47 (d, $J = 7.4$ Hz, 4H; A3+D3), 8.40 (t, 1H; E4), 7.91 (m, 4H; A4+D4), 7.35 (m, 4H; A6+D6), 7.15 ppm (m, 4H; A5+D5); IR (solid): $\tilde{\nu} = 1600$ (w), 1446 (m), 1423 (m), 1392 (m), 1338 (m), 1288 (m), 1242 (w), 1161 (w), 1107 (w), 1053 (w), 902 (w), 817 (s), 786 (s), 763 (s), 648 (m), 621 (m), 551 cm^{-1} (s); MS (ESI): m/z: 793 $[M-\text{PF}_6]^+$, 324 $[M-2\text{PF}_6]^{2+}$.

[Ru(5)Cl$_3$]: A mixture of $RuCl_3 \cdot 3H_2O$ (261 mg, 1.00 mmol) and 4′-(2-thienyl)-2,2′:6′,2″-terpyridine (**5**; 315 mg, 0.100 mmol) in EtOH (200 mL) was heated at reflux for 2 h. The reaction mixture was cooled and the brown solid that formed was collected by filtration. The crude [Ru(**5**)Cl$_3$] was washed with ethanol, dried and used without further purification.

[Ru(4)(5)][PF$_6$]$_2$: This complex was obtained as a red solid by following the method described for [Ru(tpy)(**3**)][PF$_6$]$_2$ but using 4′-chloro-2,2′:6′,2″-terpyridine (**4**; 54.0 mg, 0.202 mmol) and [Ru(**5**)Cl$_3$] (108 mg, 0.207 mmol). Yield: 120.7 mg (61.3%); ^{1}H NMR (300 MHz, CD_3CN): $\delta = 8.92$ (s, 2H; E3), 8.83 (s, 2H; B3), 8.65 (d, $J = 8.1$ Hz, 2H; D3), 8.49 (d, $J = 8.1$ Hz, 2H; A3), 8.18 (dd, $J = 1.1$, 3.7 Hz, 1H; F3), 7.94 (dt, $J = 1.1$, 8.1 Hz, 4H; A4+D4), 7.83 (dd, $J = 1.1$, 5.1 Hz, 1H; F5), 7.46 (d, $J = 5.5$ Hz, 2H; A6), 7.42 (dd, 1H; F4), 7.38 (d, $J = 5.5$ Hz, 2H; D6), 7.19 (ddd, 2H; A5), 7.17 ppm (ddd, 2H; D5); IR (solid): $\tilde{\nu} = 1595$ (w), 1539 (w), 1427 (m), 1342 (s), 1288 (m), 1245 (m), 1114 (w), 1029 (w), 825 (s), 786 (s), 756 (m), 702 (m), 651 (m), 555 (s), 528 cm^{-1} (m); MS (ESI): m/z: 829/831 $[M-\text{PF}_6]^+$, 343/342 $[M-2\text{PF}_6]^{2+}$.

[Ru(2)$_2$][PF$_6$]$_2$: A mixture of **2** (63.6 mg, 0.186 mmol), $RuCl_3 \cdot 3H_2O$ (24.3 mg, 0.093 mmol) and *N*-ethylmorpholine (4 drops) in ethane-1,2-diol (10 mL) was heated in a modified domestic microwave oven at 600 W for 4 min to give a clear red solution. The product was precipitated as a red solid by the addition of aqueous NH_4PF_6. Yield: 87.9 mg (88.2%); ^{1}H NMR (300 MHz, CD_3CN): $\delta = 8.93$ (s, 4H; B3), 8.63 (d, $J = 7.7$ Hz, 4H; A3), 7.72 (t, $J = 7.7$ Hz, 4H; A4), 7.40 (d, $J = 5.1$ Hz, 4H; A6), 7.15 (t, $J = 7.0$ Hz, 4H; A5), 7.12 (d, $J = 2.2$ Hz, 4H; C2), 6.58 ppm (t, 2H; C4); IR (solid): $\tilde{\nu} = 3078$ (w), 1604 (m), 1535 (w), 1461 (m), 1411 (m), 1323 (m), 1215 (m), 1149 (m), 1026 (m), 972 (m), 833 (s), 786 (s), 752 (m), 729 (m), 690 (m), 648 (m), 551 (m), 528 cm^{-1} (m); MS (ESI): m/z: 929 $[M-\text{PF}_6]^+$, 392 $[M-2\text{PF}_6]^{2+}$.

[Ru(tpy)(2)][PF$_6$]$_2$: This complex was prepared by following the method described for [Ru(tpy)(**3**)][PF$_6$]$_2$ using **2** (35.3 mg, 0.103 mmol) and [Ru(tpy)Cl$_3$] (45.6 mg, 0.103 mmol). The product was precipitated as an orange solid by the addition of aqueous NH_4PF_6; chromatographic purification was not required. Yield: 61.2 mg (61.6%); ^{1}H NMR (300 MHz, CD_3CN): $\delta = 8.88$ (s, 2H; B3), 8.71 (d, $J = 8.1$ Hz, 2H; E3), 8.58 (d, $J = 7.7$ Hz, 2H; A3), 8.46 (d, $J = 7.7$ Hz, 2H; D3), 8.37 (t, $J = 8.1$ Hz, 1H; E4), 7.88 (t+t, $J = 1.8$, 8.1 Hz, 4H; A4+D4), 7.37 (d, $J = 5.9$ Hz, 2H; A6), 7.30 (d, $J = 5.5$ Hz, 2H; D6), 7.12 (m, 4H; A5+D5), 7.09 (d, $J = 1.8$ Hz, 2H; C2), 6.55 ppm (t, 1H; C4); IR (solid): $\tilde{\nu} = 3325$ (w), 1600 (m), 1535 (m), 1465 (m), 1415 (m), 1245 (m), 1161 (m), 1006 (w), 817 (s), 783 (s), 767 (s), 690 (m), 644 (m), 551 (m), 516 cm^{-1} (s); MS (ESI): m/z: 821 $[M-\text{PF}_6]^+$, 338 $[M-2\text{PF}_6]^{2+}$.

[Ru(2)(5)][PF$_6$]$_2$: This complex was obtained as a red solid by following the method described for [Ru(tpy)(**2**)][PF$_6$]$_2$ using **2** (32.5 mg,

0.095 mmol) and [Ru(**5**)Cl_3] (50.2 mg, 0.096 mmol). Yield: 78.3 mg (78.6%); ^{1}H NMR (300 MHz, CD_3CN): δ = 8.92 (s, 4H; B3+E3), 8.65 (d, J = 7.7 Hz, 2H; D3), 8.62 (d, J = 7.7 Hz, 2H; A3), 8.18 (dd, J = 1.1, 3.7 Hz, 1H; F3), 7.94 (dt, J = 1.5, 7.7 Hz, 2H; D4), 7.92 (dt, J = 1.5, 7.7 Hz, 2H; A4), 7.83 (dd, J = 1.1, 5.2 Hz, 1H; F5), 7.43 (d, J = 5.5 Hz, 2H; D6), 7.42 (dd, 1H; F4), 7.41 (d, J = 5.5 Hz, 2H; A6), 7.17 (m, 4H; A5+D5), 7.13 (d, J = 2.2 Hz, 2H; C2), 6.59 ppm (t, J = 2.2 Hz, 1H; C4); IR (solid): $\tilde{\nu}$ = 1604 (m), 1539 (w), 1465 (m), 1411 (m), 1323 (w), 1288 (w), 1245 (w), 1149 (m), 1087 (w), 1006 (w), 817 (s), 786 (s), 752 (m), 713 (m), 651 (m), 621 (m), 551 cm^{-1} (m); MS (ESI): m/z: 903 $[M-PF_6]^+$, 379 $[M-2PF_6]^{2+}$.

[Os(2)$_2$][PF$_6$]$_2$: This complex was obtained as a purple solid by following the method described for [Ru(**2**)$_2$][PF_6]$_2$ using **2** (58.7 mg, 0.172 mmol), K_2OsCl_6 (27.8 mg, 0.089 mmol) and *N*-ethylmorpholine (9 drops) in ethane-1,2-diol (10 mL). Yield: 85.9 mg (86.0%); ^{1}H NMR (300 MHz, CD_3CN): δ = 8.95 (s, 4H; B3), 8.61 (d, J = 8.1 Hz, 4H; A3), 7.77 (dt, J = 1.5, 7.7 Hz, 4H; A4), 7.26 (d, J = 5.9 Hz, 4H; A6), 7.08 (ddd, 4H; A5), 7.10 (d, J = 1.8 Hz, 4H; C2), 6.51 ppm (t, 2H; C4); IR (solid): $\tilde{\nu}$ = 3052 (w), 1600 (m), 1523 (m), 1461 (m), 1419 (m), 1280 (m), 1245 (m), 1153 (w), 1130 (m), 1087 (m), 1026 (w), 1002 (m), 937 (m), 833 (s), 783 (s), 729 (m), 644 (m), 536 (m), 513 cm^{-1} (m); MS (ESI): m/z: 1018 $[M-PF_6]^+$, 437 $[M-2PF_6]^{2+}$.

[Os(2)(5)][PF$_6$]$_2$: This complex was prepared by following the method described for [Ru(**2**)(**5**)][PF_6]$_2$ using **2** (30.0 mg, 0.088 mmol) and [Os(**5**)Cl_3] (54.0 mg, 0.088 mmol) in ethane-1,2-diol (10 mL). Purification of the crude product by column chromatography (SiO_2; MeCN/saturated aqueous KNO_3/H_2O, 7:2:2) gave [Os(**2**)(**5**)][PF_6]$_2$ as a brown solid. Yield: 77.2 mg (77.3%); ^{1}H NMR (300 MHz, CD_3CN): δ = 8.95 (s, 4H; B3+D3), 8.63 (d, J = 7.4 Hz, 2H; D3), 8.61 (d, J = 7.4 Hz, 2H; A3), 8.10 (dd, J = 1.1, 3.7 Hz, 1H; F3), 7.80 (dt, J = 1.5, 7.7 Hz, 2H; D4), 7.79 (dt, J = 1.5, 8.08 Hz, 2H; A4), 7.72 (dd, J = 1.1, 5.2 Hz, 1H; F5), 7.42 (dd, J = 3.7, 5.1 Hz, 1H; F4), 7.30 (d, J = 5.1 Hz, 2H; A6), 7.29 (d, J = 5.1 Hz, 2H; D6), 7.10 (m, 4H; A5+D5), 7.10 (d, J = 2.2 Hz, 2H; C2), 6.52 ppm (t, 1H; C4); IR (solid): $\tilde{\nu}$ = 3066 (w), 1604 (m), 1581 (m), 1523 (m), 1465 (m), 1427 (m), 1396 (m), 1361 (m), 1334 (m), 1284 (m), 1245 (m), 1153 (w), 1076 (w), 1026 (w), 825 (s), 783 (s), 752 (m), 713 (m), 651 (m), 621 (m), 551 cm^{-1} (m); MS (ESI): m/z: 992 $[M-PF_6]^+$, 424 $[M-2PF_6]^{2+}$.

[(tpy)Ru(6){Ru(tpy)}$_2$][PF$_6$]$_6$: [Ru(tpy)(**2**)][PF_6]$_2$ (18.0 mg, 0.019 mmol), dry K_2CO_3 (200 mg, 1.45 mmol) and [Ru(tpy)(**4**)][PF_6]$_2$ (39.0 mg, 0.044 mmol) were dissolved in dry acetonitrile (10 mL) and the mixture was heated to reflux for 4 h. The product was precipitated by the addition of aqueous NH_4PF_6 and was purified by column chromatography (SiO_2; MeCN/saturated aqueous KNO_3/H_2O, 7:1:0.5). The first orange fraction to be eluted consisted of [Ru(tpy)(**4**)][PF_6]$_2$, and this was followed by a slower moving red compound that was identified as [(tpy)Ru(**6**){Ru(tpy)}$_2$][PF_6]$_6$. Yield: 17.5 mg (34.4%); ^{1}H NMR (300 MHz, CD_3CN): δ = 9.28 (s, 2H; B3), 8.76 (d, J = 8.1 Hz, 4H; A3+E3), 8.72 (d, J = 8.1 Hz, 4H; K3), 8.67 (s, 4H; H3), 8.55 (d, J = 8.1 Hz, 4H; G3), 8.50 (d, J = 8.1 Hz, 4H; D3), 8.46 (d, J = 2.2 Hz, 2H; C2), 8.45 (d, J = 7.0 Hz, 4H; J3), 8.42 (t, J = 8.1 Hz, 1H; E4), 8.37 (t, J = 8.1 Hz, 2H; K4), 8.02 (t, 1H; C4), 7.92 (dt, J = 1.5, 7.7 Hz, 2H; D4), 7.89 (dt, J = 1.5, 8.1 Hz, 2H; A4), 7.83 (dt, J = 1.5, 7.7 Hz, 4H; J4), 7.71 (dt, J = 1.5, 7.7 Hz, 4H; G4), 7.55 (d, J = 5.5 Hz, 4H; J6), 7.44 (d, J = 5.5 Hz, 2H; D6), 7.37 (d, J = 5.5 Hz, 2H; A6), 7.31 (d, J = 5.5 Hz, 4H; G6), 7.17 (dt, 2H; A5), 7.15 (dt, 2H; D5), 7.08 (ddd, 4H; G5), 7.04 ppm (ddd, 4H; J5); IR (solid): $\tilde{\nu}$ = 1604 (w), 1466 (w), 1404 (m), 1353 (m), 1288 (w), 1245 (w), 1199 (m), 1164 (w), 999 (w), 821 (s), 786 (s), 763 (s), 690 (m), 551 cm^{-1} (m); MS (ESI): m/z: 1194 $[M-2PF_6]^{2+}$, 748 $[M-3PF_6]^{3+}$, 525 $[M-4PF_6]^{4+}$.

[(5)Ru(6){Ru(tpy)}$_2$][PF$_6$]$_6$: The method was as described for [(tpy)Ru(**6**){Ru(tpy)}$_2$][PF_6]$_6$ using [Ru(**5**)(**2**)][PF_6]$_2$ (38.6 mg, 0.037 mmol) and [Ru(tpy)(**4**)][PF_6]$_2$ (69.8 mg, 0.078 mmol) in MeCN (10 mL). Chromatographic separation (SiO_2; MeCN/saturated aqueous KNO_3/H_2O, 7:1:0.5) resulted in orange [Ru(tpy)(**4**)][PF_6]$_2$ as the first fraction, red [Ru(**5**)(**2**)][PF_6]$_2$ as the second band, and a very slow moving red band from which a red solid was isolated that was characterised as [(**5**)Ru(**6**){Ru(tpy)}$_2$][PF_6]$_6$. Yield: 52.0 mg (50.8%); ^{1}H NMR (300 MHz, CD_3CN): δ = 9.30 (s, 2H; B3), 8.95 (s, 2H; E3), 8.77 (d, J = 8.1 Hz, 2H; A3), 8.73 (d, J = 8.1 Hz, 4H; K3), 8.68 (s, 4H; H3), 8.67 (d, J = 8.1 Hz, 2H; D3), 8.55 (d, J = 8.1 Hz, 4H; G3), 8.47 (d, J = 2.2 Hz, 2H; C2), 8.47 (d, J = 7.0 Hz, 4H; J3), 8.38 (t, J = 8.1 Hz, 2H; K4), 8.20 (dd, J = 1.1, 3.7 Hz, 1H; F3), 8.03 (t, 1H; C4), 7.95 (dt, J = 1.5, 7.7 Hz, 2H; D4), 7.92 (dt, J = 1.5, 8.1 Hz, 2H; A4), 7.85 (dt, J = 1.5, 7.7 Hz, 4H; J4), 7.85 (dd, J = 1.1, 5.1 Hz, 1H; F5), 7.72 (dt, J = 1.5, 7.7 Hz, 4H; G4), 7.55 (d, J = 5.5 Hz, 4H; J6), 7.48 (d, J = 5.5 Hz, 2H; A6), 7.47 (d, J = 5.5 Hz, 2H; D6), 7.43 (dd, J = 3.7, 5.1 Hz, 1H; F4), 7.33 (d, J = 5.5 Hz, 4H; G6), 7.19 (m, 4H; A5+D5), 7.07 ppm (m, 8H; G5+J5); IR (solid): $\tilde{\nu}$ = 1604 (w), 1585 (w), 1446 (w), 1404 (m), 1353 (m), 1288 (w), 1242 (w), 1195 (m), 1164 (w), 1026 (w), 999 (w), 829 (s), 786 (s), 767 (s), 651 (m), 555 cm^{-1} (m); MS (ESI): m/z: 1234 $[M-2PF_6]^{2+}$, 774 $[M-3PF_6]^{3+}$, 545 $[M-4PF_6]^{4+}$.

[Ru((6){Ru(tpy)}$_2$)$_2$][PF$_6$]$_{10}$: A solution of [Ru(**2**)$_2$][PF_6]$_2$ (12.0 mg, 0.011 mmol) and [Ru(tpy)(**4**)][PF_6]$_2$ (45.0 mg, 0.048 mmol) in MeCN (10 mL) was treated with dry K_2CO_3 (200 mg, 1.35 mmol) and the mixture was heated to reflux for 18 h. Complexes were precipitated by the addition of aqueous NH_4PF_6. The pentanuclear product was found to bind irreversibly to silica; attempted purification by column chromatography on silica or Sephadex or by HPLC was unsuccessful. The precipitated salts were dissolved in MeCN and very slowly reprecipitated by the addition of further aqueous NH_4PF_6. The first orange-red precipitated material was collected by filtration and was found to be pure [Ru((**6**){Ru(tpy)}$_2$)$_2$][PF_6]$_{10}$. Yield: 8.9 mg (18.0%); ^{1}H NMR (500 MHz, CD_3CN): δ = 9.34 (s, 4H; B3), 8.80 (d, J = 8.1 Hz, 4H; A3), 8.71 (d, J = 8.1 Hz, 8H; K3), 8.69 (s, 8H; H3), 8.56 (d, J = 8.1 Hz, 8H; G3), 8.48 (d, J = 2.2 Hz, 4H; C2), 8.45 (d, J = 7.0 Hz, 8H; J3), 8.40 (t, 4H; K4), 8.05 (t, 2H; C4), 7.93 (dt, J = 1.5, 8.1 Hz, 4H; A4), 7.83 (dt, J = 1.5, 7.7 Hz, 8H; J4), 7.70 (dt, J = 1.5, 7.7 Hz, 8H; G4), 7.56 (d, J = 5.5 Hz, 8H; J6), 7.50 (d, J = 5.5 Hz, 4H; A6), 7.31 (d, J = 5.5 Hz, 8H; G6), 7.09 (dt, 4H; A5), 7.07 (ddd, 8H; G5), 7.03 ppm (ddd, 8H; J6); IR (solid): $\tilde{\nu}$ = 1604 (w), 1542 (w), 1454 (w), 1404 (m), 1357 (w), 1288 (w), 1199 (m), 1154 (w), 1002 (w), 825 (s), 786 (s), 763 (s), 651 (m), 551 cm^{-1} (s); MS (ESI): m/z: 2104 $[M-2PF_6]^{2+}$, 1353 $[M-3PF_6]^{3+}$, 979 $[M-4PF_6]^{4+}$, 754 $[M-5PF_6]^{5+}$, 604 $[M-6PF_6]^{6+}$.

[(5)Os(6){Ru(tpy)}$_2$][PF$_6$]$_6$: This complex was obtained as an orange-brown solid by following the method described for the analogous complex [(**5**)Ru(**6**){Ru(tpy)}$_2$][PF_6]$_6$ but using [Os(**5**)(**2**)][PF_6]$_2$ (35.0 mg, 0.030 mmol) and [Ru(tpy)(**4**)][PF_6]$_2$ (58.1 mg, 0.062 mmol). Yield: 32.7 mg (38.3%); ^{1}H NMR (300 MHz, CD_3CN): δ = 9.30 (s, 2H; B3), 8.96 (s, 2H; E3), 8.75 (d, J = 8.1 Hz, 2H; A3), 8.72 (d, J = 8.1 Hz, 4H; K3), 8.67 (s, 4H; H3), 8.64 (d, J = 8.1 Hz, 2H; D3), 8.55 (d, J = 8.1 Hz, 4H; G3), 8.46 (d, J = 8.1 Hz, 4H; J3), 8.44 (d, J = 2.2 Hz, 2H; C2), 8.38 (4, J = 8.1 Hz, 2H; K4), 8.10 (dd, J = 1.1, 3.7 Hz, 1H; F3), 7.95 (t, 1H; C4), 7.84 (dt, J = 1.5, 7.7 Hz, 4H; J4), 7.80 (dt, J = 1.5, 7.7 Hz, 2H; D4), 7.78 (dt, J = 1.5, 8.1 Hz, 2H; A4), 7.73 (dd, J = 1.1, 5.1 Hz, 1H; F5), 7.72 (dt, J = 1.5, 7.7 Hz, 4H; G4), 7.56 (d, J = 5.5 Hz, 4H; J6), 7.42 (dd, J = 3.7, 5.1 Hz, 1H; F4), 7.34 (d, J = 5.5 Hz, 2H; A6), 7.33 (d, J = 5.5 Hz, 2H; D6), 7.32 (d, J = 5.5 Hz, 4H; G6), 7.12 (dt, 2H; A5), 7.10 (dt, J = 1.1, 7.3 Hz, 2H; D5), 7.08 (dt, J = 1.1, 7.3 Hz, 4H; G5), 7.05 ppm (dt, J = 1.1, 7.3 Hz, 4H; J5); IR (solid): $\tilde{\nu}$ = 1604 (w), 1434 (w), 1396 (m), 1357 (s), 1284 (m), 1245 (m), 1199 (m), 1164 (w), 1126 (w), 1029 (w), 999 (w), 825 (s), 786 (s), 763 (s), 651 (m), 551 cm^{-1} (s); MS (ESI): m/z: 1279 $[M-2PF_6]^{2+}$, 804 $[M-3PF_6]^{3+}$, 567 $[M-4PF_6]^{4+}$.

[(5)Os(6){Ru(5)}$_2$][PF$_6$]$_6$: This complex was obtained as an orange-brown solid by following the method described for [(**5**)Ru(**6**){Ru(tpy)}$_2$][PF_6]$_6$ using [Os(**5**)(**2**)][PF_6]$_2$ (15.1 mg, 0.013 mmol) and [Ru(**5**)(**4**)][PF_6]$_2$ (30.5 mg, 0.031 mmol). Yield: 12.7 mg (32.4%); ^{1}H NMR (500 MHz, CD_3CN): δ = 9.35 (s, 2H; B3), 8.97 (s, 2H; E3), 8.90 (s, 4H; K3), 8.78 (d, J = 8.1 Hz, 4H; A3), 8.72 (s, 4H; H3), 8.64 (d, J = 8.8 Hz, 2H; D3), 8.62 (d, J = 8.4 Hz, 4H; J3), 8.59 (d, J = 8.1 Hz, 4H; G3), 8.46 (d, J = 1.8 Hz, 2H; C2), 8.16 (dd, J = 1.1, 3.7 Hz, 2H; L3), 8.10 (dd, J = 1.1, 3.7 Hz, 1H; F3), 7.99 (t, 1H; C4), 7.85 (dt, J = 1.5, 8.1 Hz, 4H; J4), 7.81 (dd, J = 1.1, 5.1 Hz, 2H; L5), 7.80 (dt, J = 1.5, 7.7 Hz, 2H; D4), 7.77 (dt, J = 1.5, 8.08 Hz, 2H; A4), 7.73 (dd, J = 1.1, 5.1 Hz, 1H; F5), 7.71 (dt, J = 1.5, 8.4 Hz, 4H; G4), 7.59 (d, J = 5.1 Hz, 4H; J6), 7.42 (1H; F4), 7.41 (2H; L4), 7.40 (d, J = 5.1 Hz, 4H; G6), 7.34 (d, J = 5.5 Hz, 2H; D6), 7.33 (d, J = 5.5 Hz, 2H; A6), 7.11 (ddd, 2H; A5), 7.09 (ddd, 2H; D5), 7.08 (dt, 4H; G5), 7.05 ppm (dt, 4H; J5); IR (solid): $\tilde{\nu}$ = 1612 (w), 1454 (w), 1396

(m), 1357 (m), 1288 (w), 1199 (m), 1154 (w), 1026 (w), 1002 (w), 825 (s), 786 (s), 752 (m), 725 (m), 651 (m), 551 (s), 528 cm^{-1} (m); MS (ESI): *m/z*: 1361 $[M-2PF_6]^{2+}$, 859 $[M-3PF_6]^{3+}$, 608 $[M-4PF_6]^{4+}$.

$[Os((6)\{Ru(5)\}_2)_2][PF_6]_{10}$: This complex was obtained as an orange-brown solid by following the method described for $[Ru((\mathbf{6})\{Ru(tpy)\}_2)_2][PF_6]_{10}$ using $[Os(\mathbf{2})_2][PF_6]_2$ (14.0 mg, 0.012 mmol) and $[Ru(\mathbf{5})(\mathbf{4})][PF_6]_2$ (50.2 mg, 0.052 mmol). Yield: 12.8 mg (21.6%); ^1H NMR (500 MHz, CD_3CN): $\delta = 9.43$ (s, 4H; B3), 8.90 (s, 8H; K3), 8.82 (d, $J = 8.1$ Hz, 8H; A3), 8.74 (s, 8H; H3), 8.61 (d, $J = 8.1$ Hz, 16H; J3+G3), 8.49 (d, $J = 1.8$ Hz, 4H; C2), 8.16 (d, $J = 3.7$ Hz, 4H; L3), 8.03 (t, 2H; C4), 7.85 (dt, $J = 1.5$, 8.1 Hz, 8H; J4), 7.81 (dd, $J = 1.1$, 5.1 Hz, 4H; L5), 7.77 (t, $J = 7.7$ Hz, 4H; A4), 7.69 (dt, $J = 1.1$, 7.7 Hz, 8H; G4), 7.62 (d, $J = 5.5$ Hz, 8H; J6), 7.40 (dd, $J = 3.7$, 5.1 Hz, 4H; L4), 7.40 (d, $J = 5.5$ Hz, 8H; G6), 7.38 (d, $J = 5.5$ Hz, 2H; A6), 7.12 (t, 4H; A5), 7.07 (t, 4H; G5), 7.03 ppm (dt, 4H; J5); IR (solid): $\tilde{\nu} = 1608$ (w), 1585 (w), 1465 (w), 1400 (m), 1353 (m), 1284 (w), 1199 (m), 1152 (w), 1087 (m), 1026 (m), 1002 (w), 829 (s), 786 (s), 752 (m), 729 (m), 651 (m), 555 (s), 520 cm^{-1} (m); MS (ESI): *m/z*: 1493 $[M-3PF_6]^{3+}$, 1083 $[M-4PF_6]^{4+}$, 837 $[M-5PF_6]^{5+}$, 674 $[M-6PF_6]^{6+}$.

Acknowledgements

We thank the Schweizerischer Nationalfonds zur Förderung der Wissenschaftlichen Forschung, the University of Basel and the FIRB project (No. RBNE019H9K, "Molecular Manipulation for Nanometric Devices") from MIUR, Italy, for financial support.

[1] a) E. C. Constable, in *Comprehensive Coordination Chemistry II*, *Vol. 7* (Eds.: M. Fujita, A. Powell, C. Creutz; Series Eds.: J. A. McCleverty, T. J. Meyer), Elsevier, Oxford, **2003**, pp. 263–302; b) C. N. Moorefield, E. He, G. R. Newkome, *Chem. Rev.* **1999**, *99*, 1689–1746.

[2] a) A. Juris, M. Venturi, P. Ceroni, V. Balzani, S. Campagna, S. Serroni, *Collect. Czech. Chem. Commun.* **2001**, *66*, 1–32; b) J. F. Stoddart, T. Welton, *Polyhedron* **1999**, *18*, 3575–3591; c) S. Serroni, S. Campagna, G. Denti, A. Juris, M. Venturi, V. Balzani, in *Advances in Dendritic Macromolecules*, *Vol. 3* (Ed.: G. R. Newkome), Jai Press, Greenwich, **1996**, pp. 193–228; d) M. Venturi, S. Serroni, A. Juris, S. Campagna, V. Balzani, in *Dendrimers* (Ed.: F. Vögtle), Springer-Verlag, Berlin, **1998**, pp. 193–228; e) A. Hearshow, A. T. Hutton, J. R. Moss, K. J. Naidoo, in *Advances in Dendritic Macromolecules*, *Vol. 4* (Ed.: G. R. Newkome), Jai Press, Stamford, **1999**, pp. 1–60.

[3] E. C. Constable, *Chem. Commun.* **1997**, 1073–1080.

[4] a) C. Amatore, Y. Bouret, E. Maisonhaute, J. I. Goldsmith, H. D. Abruna, *Chem. Eur. J.* **2001**, *7*, 2206–2226; b) H. F. Chow, I. Y. K. Chan, P. S. Fung, T. K. K. Mong, M. F. Nongrum, *Tetrahedron* **2001**, *57*, 1565–1572; c) H. F. Chow, I. Y. K. Chan, D. T. W. Chan, R. W. M. Kwok, *Chem. Eur. J.* **1996**, *2*, 1085–1091.

[5] D. Armspach, M. Cattalini, E. C. Constable, C. E. Housecroft, D. Phillips, *Chem. Commun.* **1996**, 1823–1824.

[6] a) V. Balzani, P. Ceroni, A. Juris, M. Venturi, S. Campagna, F. Puntoriero, S. Serroni, *Coord. Chem. Rev.* **2001**, *219*, 545–572; b) S. Campagna, C. Di Pietro, F. Loiseau, B. Maubert, N. McClenaghan, R. Passalacqua, F. Puntoriero, V. Ricevuto, S. Serroni, *Coord. Chem. Rev.* **2002**, *229*, 67–74.

[7] a) E. C. Constable, M. Cattalini, O. Eich, C. E. Housecroft, L. A. Johnston, I. Poleschak, *Polym. Mater. Sci. Eng.* **1999**, *80*, 268; b) E. C. Constable, C. E. Housecroft, I. Poleschak, *Inorg. Chem. Commun.* **1999**, *2*, 565–568; c) E. C. Constable, C. E. Housecroft, M. Neuburger, I. Poleschak, M. Zehnder, *Polyhedron* **2003**, *22*, 93–108; d) E. C. Constable, R. Frantz, C. E. Housecroft, J. Lacour, A. Mahmood, *Inorg. Chem.* **2004**, *43*, 4817–4819; e) E. C. Constable, P. Harverson, C. E. Housecroft, *J. Chem. Soc. Dalton Trans.* **1999**, 3693–3700; f) E. C. Constable, P. Harverson, M. Oberholzer, *Chem. Commun.* **1996**, 1821–1822.

[8] a) A. Juris, L. Prodi, *New J. Chem.* **2001**, *25*, 1132–1135; b) A. Boerje, O. Koethe, A. Juris, *New J. Chem.* **2001**, *25*, 191–193; c) A. Boerje, O. Koethe, A. Juris, *J. Chem. Soc. Dalton Trans.* **2002**, 843–848; d) D. Tzalis, Y. Tor, *Chem. Commun.* **1996**, 1043–1045.

[9] E. C. Constable, R. W. Handel, C. E. Housecroft, A. F. Morales, L. Flamigni, F. Barigelletti, *Dalton Trans.* **2003**, 1220–1222.

[10] V. Balzani, S. Campagna, G. Denti, A. Juris, S. Serroni, M. Venturi, *Acc. Chem. Res.* **1998**, *31*, 26–34.

[11] A. Börje, O. Kothe, A. Juris, *J. Chem. Soc. Dalton Trans.* **2002**, 843–848.

[12] F. Barigelletti, L. Flamigni, *Chem. Soc. Rev.* **2000**, *29*, 1–12.

[13] E. C. Constable, C. E. Housecroft, M. Cattalini, D. Phillips, *New J. Chem.* **1998**, *22*, 193–200.

[14] F. Kröhnke, *Synthesis* **1976**, 1–24.

[15] W. Spahni, G. Calzaferri, *Helv. Chim. Acta* **1984**, *67*, 450–454.

[16] S. Encinas, L. Flamigni, F. Barigelletti, E. C. Constable, C. E. Housecroft, E. R. Schofield, E. Figgemeier, D. Fenske, M. Neuburger, J. G. Vos, M. Zehnder, *Chem. Eur. J.* **2002**, *8*, 137–150.

[17] a) E. C. Constable, D. Morris, S. Carr, *New J. Chem.* **1998**, *22*, 287–294; b) C. O. Dietrich-Buchecker, J. P. Sauvage, J. P. Kintzinger, P. Maltese, C. Pascard, J. Guilhem, *New J. Chem.* **1992**, *16*, 931–942; c) C. Dietrich-Buchecker, C. Hemmert, J. P. Sauvage, *New J. Chem.* **1990**, *14*, 603–605.

[18] M. Grätzel, *Nature* **2001**, *414*, 338–344.

[19] a) J. Hjelm, E. C. Constable, E. Figgemeier, A. Hagfeldt, R. Handel, C. E. Housecroft, E. Mukhtar, E. Schofield, *Chem. Commun.* **2002**, 284–285; b) E. C. Constable, C. E. Housecroft, E. R. Schofield, S. Encinas, N. Armaroli, F. Barigelletti, L. Flamigni, E. Figgemeier, J. G. Vos, *Chem. Commun.* **1999**, 869–870.

[20] a) E. C. Constable, *Inorg. Chim. Acta* **1986**, *117*, L33–L34; b) E. C. Constable, T. A. Leese, *Inorg. Chim. Acta* **1988**, *146*, 55–58.

[21] E. C. Constable, *Metals and Ligand Reactivity*, VCH, Weinheim, **1995**.

[22] A. S. Abd-El-Aziz, C. R. de Denus, M. J. Zaworotko, L. R. MacGillivray, *J. Chem. Soc. Dalton Trans.* **1995**, 3375–3393.

[23] J. P. Sauvage, J. P. Collin, J. C. Chambron, S. Guillerez, C. Coudret, V. Balzani, F. Barigelletti, L. De Cola, L. Flamigni, *Chem. Rev.* **1994**, *94*, 993–1019.

[24] According to a different approach, one might compare the behaviour of equimolar solutions; see, for instance, Serin et al. in ref. [25] below. In this way, an *apparent* gain in luminescence intensity for the dendritic case may be registered, as compared to what happens in the component model, simply because of the increased absorbance within the dendrimer, that is, because of absorption of a greater number of photons. However, given that the luminescence quantum yield refers to photons emitted over photons absorbed (per unit time), it seems more appropriate to deal with isoabsorbing conditions.

[25] J. M. Serin, D. W. Brousmiche, J. M. J. Fréchet, *J. Am. Chem. Soc.* **2002**, *124*, 11848–11849.

[26] a) T. Förster, *Discuss. Faraday Soc.* **1959**, *27*, 7; b) J. R. Lakowicz, *Principles of Fluorescence Spectroscopy*, Plenum, New York, **1999**.

[27] L. Hammarström, F. Barigelletti, L. Flamigni, N. Armaroli, A. Sour, J. P. Collin, J. P. Sauvage, *J. Am. Chem. Soc.* **1996**, *118*, 11972–11973.

[28] K. Nakamaru, *Bull. Chem. Soc. Jpn.* **1982**, *55*, 2967.

[29] J. N. Demas, G. A. Crosby, *J. Phys. Chem.* **1971**, *75*, 991–1024.

Received: February 2, 2005
Published online: April 28, 2005